

AHP: Learning to Negative Sample for Hyperedge Prediction

Hyunjin Hwang*
KAIST AI
Seoul, South Korea
hyunjinhwang@kaist.ac.kr

Seungwoo Lee*
KAIST EE
Daejeon, South Korea
ksalsw1996@kaist.ac.kr

Chanyoung Park
KAIST ISysE & AI
Daejeon, South Korea
cy.park@kaist.ac.kr

Kijung Shin
KAIST AI & EE
Seoul, South Korea
kijungs@kaist.ac.kr

ABSTRACT

Hypergraphs (i.e., sets of hyperedges) naturally represent group relations (e.g., researchers co-authoring a paper and ingredients used together in a recipe), each of which corresponds to a hyperedge (i.e., a subset of nodes). Predicting future or missing hyperedges bears significant implications for many applications (e.g., collaboration and recipe recommendation). What makes hyperedge prediction particularly challenging is the vast number of non-hyperedge subsets, which grows exponentially with the number of nodes. Since it is prohibitive to use all of them as negative examples for model training, it is inevitable to sample a very small portion of them, and to this end, heuristic sampling schemes have been employed. However, trained models suffer from poor generalization capability for examples of different natures. In this paper, we propose AHP, an adversarial training-based hyperedge-prediction method. It learns to sample negative examples without relying on any heuristic schemes. Using six real hypergraphs, we show that AHP generalizes better to negative examples of various natures. It yields up to **28.2% higher AUROC** than the best existing methods and often even outperforms its variants with sampling schemes tailored to test sets.

CCS CONCEPTS

• **Computing methodologies** → **Neural networks**; • **Information systems** → **Recommender systems**.

KEYWORDS

hypergraph; hyperedge prediction; link prediction; recommendation; adversarial training

ACM Reference Format:

Hyunjin Hwang, Seungwoo Lee, Chanyoung Park, and Kijung Shin. 2022. AHP: Learning to Negative Sample for Hyperedge Prediction. In *Proceedings of the 45th International ACM SIGIR Conference on Research and Development in Information Retrieval (SIGIR '22)*, July 11–15, 2022, Madrid, Spain. ACM, New York, NY, USA, 6 pages. <https://doi.org/10.1145/XXXXXX.XXXXXX>

1 INTRODUCTION

Group relations among objects are common in complex systems: (a) researchers co-authoring a paper, (b) items co-purchased by a *Equal Contribution.

Permission to make digital or hard copies of all or part of this work for personal or classroom use is granted without fee provided that copies are not made or distributed for profit or commercial advantage and that copies bear this notice and the full citation on the first page. Copyrights for components of this work owned by others than ACM must be honored. Abstracting with credit is permitted. To copy otherwise, or republish, to post on servers or to redistribute to lists, requires prior specific permission and/or a fee. Request permissions from [permissions@acm.org](https://permissions.acm.org).
SIGIR '22, July 11–15, 2022, Madrid, Spain.

© 2022 Association for Computing Machinery.
ACM ISBN 978-1-4503-8732-3/22/07...\$15.00
<https://doi.org/10.1145/XXXXXX.XXXXXX>

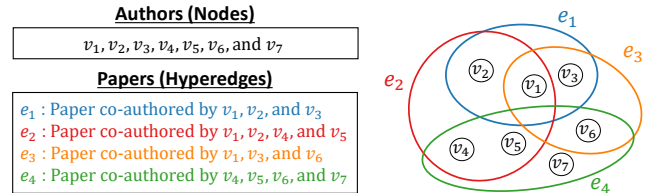


Figure 1: Collaboration data modeled as a hypergraph.

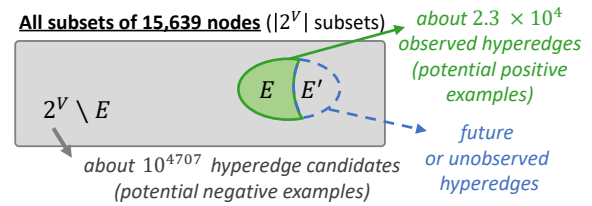


Figure 2: Venn diagram of hyperedges and candidates in the DBLP dataset. The number of candidates is extremely large.

shopper, (c) ingredients in a recipe, (d) proteins inducing a chemical reaction together, (e) drugs causing side effects when taken together, to name a few [1, 4–9, 18–21, 31]. They together are naturally modeled as a *hypergraph* (i.e., a set of hyperedges) where each *hyperedge* (i.e., a subset of nodes) indicates a group relation among the nodes in it. See Fig. 1 for an example hypergraph.

Hyperedge prediction (i.e., the task of predicting future or unobserved hyperedges) is a fundamental task with numerous applications, including collaboration/movie/recipe recommendation [24, 40, 42], chemical reaction prediction [38, 42], drug side-effect prediction [26, 33]. Thus, it has received considerable attention in the recommendation system and machine learning communities.

One of the main challenges in hyperedge prediction is the vast number of potential negative examples, i.e., subsets of nodes that are not a hyperedge. As illustrated in Fig. 2, their number is about $10^{4,707}$ in a dataset used, and formally, their number is $2^{|V|} - |E|$, where V and E are the sets of nodes and hyperedges, respectively. Thus, it is practically impossible to utilize all non-hyperedge subsets as negative examples when training machine learning models.

Therefore, it is inevitable to sample a tiny portion of potential negative examples, and to this end, existing machine-learning-based hyperedge-prediction methods [27, 32, 38, 39, 43] resort to heuristic sampling schemes. For example, a negative example is sampled by replacing half of the nodes in a hyperedge with random nodes [38].

However, we observe that models trained using such negative examples suffer from poor generalization capability. Specifically, their capability of classifying positive and negative examples heavily depends on sampling schemes used for training and test sets. Our finding obtained from state-of-the-art methods [38, 39, 43] complements the findings in [27], where rule-based and simple learning-based techniques are used to compare sampling schemes.

In this paper, we propose AHP (Adversarial training-based Hyperedge Prediction), which learns to sample negative examples without relying on heuristic sampling schemes. Its generator aims to fool its discriminator by sampling hard negative examples. We adapt a hypergraph neural network for the discriminator and design a generator simple yet well-suited to hyperedge prediction, while our training method is model agnostic. Based on experimental results, we summarize our contributions as follows:

- **Observation:** We show that heuristic sampling schemes limit the generalization ability of deep learning-based hyperedge-prediction.
- **Solution:** AHP learns to sample negative examples by adversarial training for better generalization. In terms of AUROC, AHP is up to **28.2% better** than best existing methods and up to **5.5% better** than variants with sampling schemes tailored to test sets.
- **Experiments:** We compare AHP with 3 sampling schemes and 3 recent hyperedge-prediction methods on 6 real hypergraphs. For **reproducibility**, the code and datasets used in the paper are available at <https://github.com/HyunjinHwn/SIGIR22-AHP>.

2 PRELIMINARIES

In this section, we provide some preliminaries on hyperedge prediction and hypergraph neural networks.

Basic concepts. Consider a **hypergraph** $H = (V, E)$ consisting of a set of nodes $V = \{v_1, \dots, v_{|V|}\}$ and a set of hyperedges $E = \{e_1, \dots, e_{|E|}\}$ (see Fig. 1 for an example). Each **hyperedge** $e_i \in E$ is a subset of nodes, i.e., $e_i \subseteq V$. Each (i, j) -th entry of the **incidence matrix** $A \in \mathbb{R}^{|V| \times |E|}$ of H is 1 if $v_i \in e_j$, and it is 0 otherwise. We also assume **node features** $X \in \mathbb{R}^{|V| \times d}$, where each i -th row corresponds to the d -dimensional feature of the node v_i .

Problem definition. For a given hypergraph $H = (V, E)$, the objective of hyperedge prediction is to find the **target set** $E' \subseteq 2^V \setminus E$, which typically consists of (a) unobserved hyperedges or (b) new hyperedges that will arrive in the near future. Each member of $2^V \setminus E$ is called a **hyperedge candidate** as it may belong to E' . Due to the vast number of hyperedge candidates (see Fig. 2 for an example), ranking or evaluating every candidate is computationally infeasible. Thus, hyperedge prediction is typically formulated as a classification problem below [27, 32, 38, 39, 43].

Problem 1 (Hyperedge prediction). Given a hypergraph $H = (V, E)$, node features $X \in \mathbb{R}^{|V| \times d}$, and a hyperedge candidate $c \in 2^V \setminus E$, we aim to classify whether c belongs to the target set E' or not.

Hypergraph neural networks. Hypergraph neural networks (HyperGNNs) [10, 11, 32, 37, 38] are a class of neural networks designed to perform inference on hypergraphs, and they proved effective for a number of applications [12, 22, 30, 35, 38, 41]. A representative HyperGNN is HNHN [10], which repeats (a) producing node embeddings by aggregating the embeddings of incident hyperedges and (b) producing hyperedge embeddings by aggregating the embeddings of incident nodes by using Eq. (1) for each layer $l \in \{1, \dots, L\}$.

$$X_E^{(l)} = \sigma(A^T X_V^{(l-1)} W_V^{(l)} + b_V^{(l)}), \quad X_V^{(l)} = \sigma(A X_E^{(l)} W_E^{(l)} + b_E^{(l)}), \quad (1)$$

where $W_V^{(l)}$ and $W_E^{(l)}$ are learnable weight matrices and $b_V^{(l)}$ and $b_E^{(l)}$ are learnable bias matrices. The matrix A is the incident matrix, and the initial embeddings $X_V^{(0)}$ equal to the given node features X . The function σ is a nonlinear activation function, and in Eq. (1),

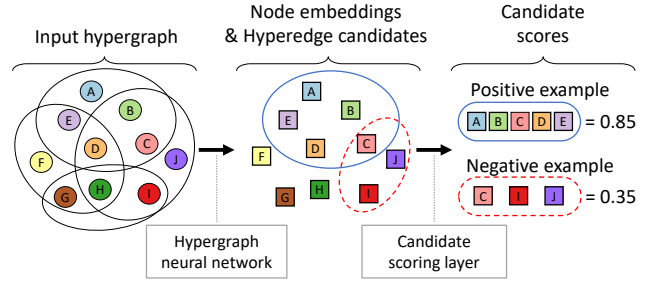


Figure 3: Hyperedge prediction using a hypergraph neural network and a candidate scoring layer.

normalization terms are omitted for simplicity. The output of HNHN is $X_V^{(L)}$, i.e., the node embeddings in the last layer, as in Fig. 3.

Candidate scoring. In order to apply hypergraph neural networks, whose output is node embeddings, to hyperedge prediction, two additional steps are required. For a given hyperedge candidate $c \in 2^V \setminus E$, the embeddings of nodes in c are pooled (for example, by being averaged) into the embedding of c . Then, the embedding is used (for example by being fed into MLP) to estimate how likely c belongs to the target set E' , as in Fig. 3.

Training and negative sampling. Based on the assumption that (unobserved or future) hyperedges in the target set E' bear similarities with (observed) hyperedges in E , the members of E are used as **positive examples**, and the members of $2^V \setminus E$ are used as **negative examples** during training. That is, the hypergraph neural network and the hyperedge scoring layer are trained so that positive examples earn higher scores and negative examples earn lower scores, as in Fig. 3. Due to the vast size of $2^V \setminus E$ (see Fig. 2 for an example), it is prohibitive to use all its members as negative examples, and it is inevitable to sample a tiny portion of them. This sampling process is called **negative sampling**. As discussed in Sect. 1, to this end, heuristic schemes are commonly used, such as:

- **Sized negative sampling (SNS):** fill a set with k random nodes.
- **Motif negative sampling (MNS):** fill a set of size k by repeatedly merging it with a random incident edge in the clique expansion.
- **Clique negative sampling (CNS):** pick a random hyperedge and replace a random constituent node with a random node that is adjacent to all other constituent nodes.

In all the sampling schemes above [27], random selection is uniform, and the size k of each negative example is drawn iid from the hyperedge size distribution in the input hypergraph. As discussed in Sect. 1 and demonstrated in Sect. 4, these sampling schemes limit the generalization capability of hyperedge-prediction methods.

3 PROPOSED METHOD

In this section, we propose AHP (Adversarial training-based Hyperedge Prediction), which learns to negative sample, without relying on heuristic negative sampling schemes, for deep learning-based hyperedge prediction. AHP consists of (a) a **generator** for sampling negative examples and (b) a **discriminator** for candidate scoring, which are **trained adversarially**, as depicted in Fig. 4.

Challenges. It should be noted that our objective of adversarial training is different from the typical one (i.e., to train a generator). For successful hyperedge prediction, the power of the generator

needs to be within an appropriate range. If the generator is too weak, it produces only trivial negative samples, which are not helpful to effective training of the discriminator. On the other hand, if it is powerful enough to produce positive examples or those in the target set, it loses its role of sampling negative examples.

Generator. Due to this reason, for the generator of AHP, using our simple architecture (described below) resulted in more accurate hyperedge prediction than adapting advanced architectures (e.g., [34]), in our preliminary study. The generator of AHP consists of a simple multi-layer perceptron (MLP) with three layers and LeakyReLU as activation functions between them. Specifically, the generator first draws k , the size of a negative example, from the size distribution of positive examples. Then, its MLP model generates a vector for node membership from a random Gaussian noise. Lastly, it selects *Top-k* nodes in the vector that together compose a negative example, which is then fed into the discriminator.

Discriminator. Given a subset of nodes (i.e., a positive or negative example during training and a hyperedge candidate during inference), the discriminator measures a score that indicates how likely the nodes together form a hyperedge. For the discriminator, we use HNHN for node embedding and the *maxmin* function (i.e., element-wise maximum - element-wise minimum) followed by MLP for candidate scoring (see Sect. 2 for HNHN and candidate scoring). Intuitively, the *maxmin* function measures how diverse the embeddings of nodes are in a given subset, and the diversity may reveal important clues regarding hyperedge formation as homophily (i.e., similar nodes are more likely to form hyperedges together than dissimilar nodes) is pervasive in real-world hypergraphs [19].

Adversarial training. As depicted in Fig. 4, we train the generator G and the discriminator D adversarially, by repeating three steps for each batch S of positive examples, (1) **sample** $|S|$ negative examples using G , (2) **classify** the positive and negative examples using D , and (3) **update** G and D using gradient descent on their losses. As D aims to make the scores of positive examples larger and those of negative examples smaller, for a given hypergraph H and node features X , the loss function for D is:

$$\mathcal{L}_D = -\frac{1}{|S|} \sum_{s \in S} [D(s|H, X)] + \frac{1}{|S|} \sum_{j=1}^{|S|} [D(G(z_j)|H, X)], \quad (2)$$

where $G(z_j)$ is a negative example generated from the noise z_j . Since G aims to fool D and make it classify its negative examples as positive, the loss function for G is:

$$\mathcal{L}_G = -\frac{1}{|S|} \sum_{j=1}^{|S|} [D(G(z_j)|H, X)]. \quad (3)$$

Memory bank for training stability. Adversarial training often suffers from instability [2, 3, 28, 29], and to mitigate it, we employ a memory bank. Specifically, we maintain the “hardest” negative examples, i.e. negative examples that earned the highest scores by the discriminator in the previous iteration, and reuse them as negative examples.¹ By keeping hard negative examples, we aim to prevent the discriminator from losing its generalization ability even if the generator accidentally samples only easy negative examples.

¹With the extra negative samples M , the loss for D is $\mathcal{L}_D = -\frac{1}{|S|} \sum_{s \in S} [D(s|H, X)] + \frac{1}{|S|+|M|} \left(\sum_{j=1}^{|S|} [D(G(z_j)|H, X)] + \sum_{m \in M} [D(m|H, X)] \right)$. $|M|$ is a hyperparameter.

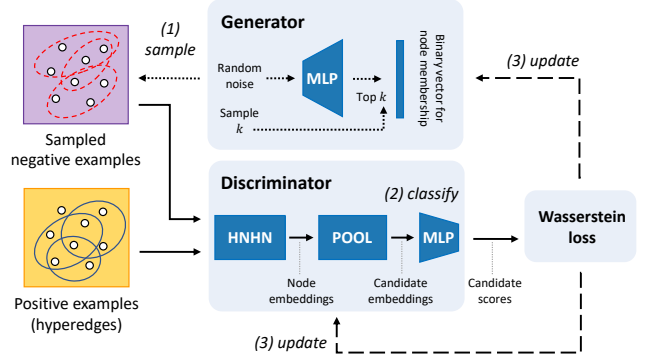


Figure 4: Training of AHP. The generator learns to sample negative examples, aiming at fooling the discriminator.

4 EXPERIMENTS

In this section, we review our experiments whose results support the effectiveness of AHP.

Experimental settings. We performed all experiments on a server with 256GB of RAM and RTX 2080 Ti GPUs, each of which has 11GB of vRAM. We split the hyperedges in each dataset into training (60%), validation (20%), and test (20%) sets. Validation and test hyperedges are unobserved and thus not used for node embedding. We also masked some (spec., 1/6) of training hyperedges during node embedding to facilitate generalization. We formed four validation and test sets by adding negative examples from SNS, MNS, CNS, and a mixture of them. We measured AUROC and AP on each test set at an epoch when AUROC averaged over four validation sets was maximized, and we reported means over five runs.

Datasets We used one **collaboration** (DBLP), three **co-citation** (Citeseer, Cora, and Pubmed), and two **authorship** (DBLP-A and Cora-A) datasets. See Appendix for some basic statistics of them.

- **Collaboration dataset:** A collaboration dataset is modeled as a hypergraph where each node is a researcher and each hyperedge is the set of (co-)authors of a paper. As in [37], we constructed the DBLP dataset from 22,964 papers (i.e., hyperedges) from 87 venues.² The papers were (co-)authored by 15,639 researchers (i.e., nodes) and available at the Aminer academic network.³ For the features of each node, we averaged the bag-of-word features from the abstracts of the papers (co-)authored by the node.
- **Co-citation datasets:** A co-citation dataset is modeled as a hypergraph where each node is a paper and each hyperedge is the set of papers cited by a paper. For the features of each node, we used the bag-of-word features from its abstract. We used three co-citation datasets: Citeseer, Cora, and Pubmed.⁴
- **Authorship datasets:** An authorship data is modeled as a hypergraph where each node is a paper and each hyperedge is the set of papers (co-)authored by a researcher. For the features of each node, we used the bag-of-word features from its abstract. We used two authorship datasets, DBLP-A⁵ and Cora-A⁶, which were also used in [10, 37].

²They belong to the following six conference categories: algorithms, database, programming, data mining, intelligence, and vision.

³<https://ifs.aminer.cn/lab-datasets/citation/DBLP-citation-network-Oct-19.tar.gz>

⁴<https://linqs.soe.ucsc.edu/data>

⁵<https://github.com/mallabiisc/HyperGCN>

⁶<https://people.cs.umass.edu/mccallum/data.html>

Table 1: Hyperedge prediction performance and standard deviation. In terms of AUROC averaged over four test sets (i.e., SNS, MNS, CNS, and S+M+C), AHP is up to 28.2% better than the best existing method and up to 5.5% better than its best variants.

Dataset	Citeseer										Cora-A									
	AUROC					AP					AUROC					AP				
	SNS	MNS	CNS	S+M+C	AVG	SNS	MNS	CNS	S+M+C	AVG	SNS	MNS	CNS	S+M+C	AVG	SNS	MNS	CNS	S+M+C	AVG
Expansion	0.663	0.781	0.331	0.588	0.591 ± 0.011	0.765	0.817	0.498	0.630	0.681 ± 0.001	0.690	0.842	0.434	0.658	0.656 ± 0.011	0.690	0.876	0.577	0.672	0.706 ± 0.020
NHP	0.991	0.701	0.510	0.817	0.751 ± 0.009	0.990	0.731	0.520	0.768	0.751 ± 0.011	0.909	0.672	0.550	0.773	0.723 ± 0.015	0.925	0.720	0.585	0.766	0.748 ± 0.019
HyperSAGNN	0.540	0.410	0.473	0.478	0.475 ± 0.019	0.627	0.455	0.497	0.507	0.521 ± 0.015	0.386	0.591	0.542	0.505	0.506 ± 0.019	0.532	0.643	0.545	0.563	0.571 ± 0.009
AHP-S	0.865	0.844	0.629	0.785	0.781 ± 0.030	0.888	0.838	0.644	0.778	0.787 ± 0.027	0.946	0.917	0.753	0.870	0.872 ± 0.011	0.951	0.896	0.770	0.857	0.869 ± 0.016
AHP-M	0.825	0.803	0.613	0.749	0.748 ± 0.029	0.837	0.797	0.639	0.749	0.756 ± 0.026	0.940	0.916	0.758	0.878	0.873 ± 0.012	0.945	0.894	0.785	0.873	0.874 ± 0.011
AHP-C	0.858	0.844	0.633	0.774	0.777 ± 0.019	0.873	0.839	0.661	0.773	0.786 ± 0.013	0.946	0.918	0.762	0.880	0.876 ± 0.014	0.949	0.896	0.792	0.875	0.878 ± 0.014
AHP-S+M+C	0.861	0.844	0.629	0.764	0.774 ± 0.014	0.873	0.835	0.653	0.753	0.779 ± 0.015	0.945	0.917	0.762	0.873	0.874 ± 0.016	0.950	0.895	0.796	0.870	0.878 ± 0.016
AHP (Proposed)	0.943	0.881	0.651	0.820	0.824 ± 0.020	0.952	0.870	0.660	0.795	0.819 ± 0.022	0.958	0.924	0.782	0.887	0.888 ± 0.014	0.957	0.898	0.796	0.878	0.882 ± 0.014

Dataset	Cora										Pubmed									
	AUROC					AP					AUROC					AP				
	SNS	MNS	CNS	S+M+C	AVG	SNS	MNS	CNS	S+M+C	AVG	SNS	MNS	CNS	S+M+C	AVG	SNS	MNS	CNS	S+M+C	AVG
Expansion	0.470	0.707	0.256	0.476	0.477 ± 0.009	0.637	0.764	0.454	0.563	0.607 ± 0.009	0.520	0.730	0.241	0.497	0.497 ± 0.015	0.675	0.755	0.44	0.565	0.612 ± 0.010
NHP	0.943	0.641	0.472	0.774	0.703 ± 0.015	0.949	0.678	0.509	0.744	0.718 ± 0.020	0.973	0.694	0.524	0.745	0.733 ± 0.004	0.973	0.656	0.513	0.678	0.707 ± 0.004
HyperSAGNN	0.617	0.527	0.494	0.540	0.545 ± 0.021	0.687	0.574	0.508	0.566	0.584 ± 0.019	0.525	0.686	0.546	0.580	0.584 ± 0.066	0.534	0.680	0.529	0.561	0.576 ± 0.050
AHP-S	0.935	0.835	0.565	0.776	0.777 ± 0.016	0.939	0.828	0.554	0.734	0.764 ± 0.025	0.904	0.837	0.535	0.759	0.759 ± 0.005	0.909	0.819	0.524	0.707	0.740 ± 0.012
AHP-M	0.919	0.836	0.573	0.782	0.777 ± 0.012	0.922	0.823	0.550	0.737	0.758 ± 0.018	0.839	0.861	0.553	0.751	0.751 ± 0.010	0.837	0.859	0.544	0.712	0.738 ± 0.017
AHP-C	0.902	0.824	0.575	0.765	0.767 ± 0.024	0.906	0.813	0.553	0.726	0.749 ± 0.040	0.786	0.839	0.555	0.726	0.727 ± 0.007	0.800	0.842	0.553	0.702	0.724 ± 0.011
AHP-S+M+C	0.917	0.830	0.570	0.769	0.771 ± 0.018	0.921	0.820	0.553	0.719	0.753 ± 0.026	0.869	0.855	0.554	0.762	0.760 ± 0.010	0.865	0.856	0.547	0.725	0.748 ± 0.008
AHP (Proposed)	0.964	0.860	0.572	0.799	0.799 ± 0.019	0.961	0.837	0.552	0.740	0.772 ± 0.035	0.917	0.840	0.533	0.763	0.763 ± 0.009	0.918	0.834	0.526	0.717	0.749 ± 0.007

Dataset	DBLP-A										DBLP									
	AUROC					AP					AUROC					AP				
	SNS	MNS	CNS	S+M+C	AVG	SNS	MNS	CNS	S+M+C	AVG	SNS	MNS	CNS	S+M+C	AVG	SNS	MNS	CNS	S+M+C	AVG
Expansion	0.634	0.826	0.350	0.603	0.603 ± 0.006	0.730	0.852	0.512	0.641	0.687 ± 0.004	0.645	0.801	0.366	0.607	0.607 ± 0.005	0.751	0.856	0.518	0.655	0.698 ± 0.004
NHP	0.966	0.623	0.555	0.721	0.716 ± 0.005	0.965	0.604	0.534	0.663	0.693 ± 0.007	0.663	0.540	0.503	0.572	0.569 ± 0.003	0.608	0.523	0.501	0.542	0.544 ± 0.002
HyperSAGNN	0.548	0.791	0.563	0.636	0.634 ± 0.007	0.686	0.805	0.552	0.655	0.675 ± 0.004	0.448	0.574	0.572	0.530	0.531 ± 0.018	0.562	0.602	0.586	0.577	0.582 ± 0.016
AHP-S	0.902	0.894	0.622	0.835	0.813 ± 0.011	0.917	0.897	0.649	0.836	0.825 ± 0.006	0.944	0.815	0.557	0.774	0.773 ± 0.003	0.944	0.811	0.546	0.728	0.757 ± 0.005
AHP-M	0.895	0.900	0.626	0.831	0.813 ± 0.012	0.910	0.904	0.656	0.833	0.826 ± 0.010	0.941	0.829	0.553	0.773	0.774 ± 0.001	0.944	0.829	0.550	0.733	0.764 ± 0.003
AHP-C	0.891	0.893	0.615	0.833	0.812 ± 0.015	0.908	0.899	0.679	0.829	0.829 ± 0.011	0.876	0.767	0.566	0.736	0.736 ± 0.002	0.875	0.751	0.563	0.705	0.723 ± 0.002
AHP-S+M+C	0.894	0.895	0.634	0.832	0.814 ± 0.011	0.911	0.901	0.680	0.835	0.832 ± 0.008	0.922	0.805	0.573	0.767	0.767 ± 0.017	0.926	0.800	0.576	0.735	0.759 ± 0.018
AHP (Proposed)	0.916	0.926	0.668	0.838	0.837 ± 0.004	0.928	0.928	0.707	0.836	0.850 ± 0.003	0.946	0.820	0.568	0.778	0.778 ± 0.002	0.947	0.815	0.561	0.735	0.764 ± 0.007

Implementation details. We implemented AHP in PyTorch and Deep Graph Library (DGL).⁷ We set the node embedding dimension to 800 for the Pubmed dataset and 400 for the other datasets, as in [10]. We used a three-layer MLP with LeakyReLU as activation functions for the generator. We set the dimension of MLP to [64, 256, 256, the number of nodes] for the Citeseer, Cora, and Cora-A datasets and to [128, 1024, 1024, the number of nodes] for the other datasets. We used a three-layer MLP with ReLU as activations functions for the classifier, and we set its dimension to [the node embedding dimension, 128, 8, 1]. The discriminator and the generator were trained alternately for the same number of epochs. We also tuned (a) the learning rates of the discriminator and the generator, (b) the normalization factors of HNHN, and (c) the size of the memory bank. See Appendix for their search space.

Baseline. As baseline approaches, we used Expansion [39], NHP [38], and HyperSAGNN [43], which are state-of-the-art methods for hyperedge prediction formulated as a classification problem. For them, we used the same node embedding dimension of AHP and used equal numbers of positive and negative examples in each epoch. We tuned their learning rates among {0.01, 0.001, 0.0001}, and we set the other hyperparameters and sampled negative examples as suggested in the original publications.⁸ We additionally

⁷<https://www.dgl.ai/>

⁸For Expansion, we used features from 2- and 3-projected graphs and sampled negative examples so that the nodes in each example form a star in the 2-projected graph.

considered four variants of AHP (AHP-S, AHP-M, AHP-C, and AHP-S+M+C) where only the learnable generator of AHP is replaced by SNS, MNS, CNS, and a mixture of them, respectively. In them, negative examples are re-sampled at each iteration, as in AHP. See Appendix for their hyperparameter search space.

Comparison with state of the arts. As shown in Table 1, AHP outperformed all state-of-the-art competitors (i.e., Expansion, NHP, and HyperSAGNN) on 19 (out of 24) and 17 test sets in terms of AUROC and AP, respectively. Moreover, **AHP performed best in all the six datasets in terms of AUROC and AP averaged over four test sets (i.e., SNS, MNS, CNS, and S+M+C).** Especially, in the DBLP dataset, AHP was **28.2% better**, in terms of average AUROC, than Expansion, which was the best existing method. The generalization ability of Expansion, NHP, and HyperSAGNN, which all rely on heuristic sampling schemes, was very limited, as seen in the fact that their AUROC was lower than 0.5 on multiple test sets.

Comparison with variants. As shown in Table 1, among the variants of AHP, one equipped with the same sampling scheme used for each test set tended to perform best. For example, in the Pubmed dataset, AHP-S, AHP-M, AHP-C, and AHP-S+M+C performed best in test sets constructed by SNS, MNS, CNS, and SNS+MNS+CNS, respectively. The results indicate that their generalization ability heavily depends on heuristic sampling schemes. **AHP performed better by up to 5.5% than all its variants in terms of AUROC and AP averaged over four test sets, in all the six datasets.**

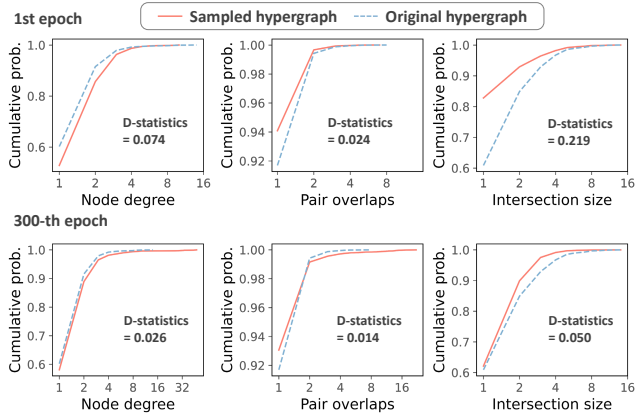


Figure 5: Comparison of the hyperedges and the negative examples from the generator on the Cora-A dataset. Note that they became closer w.r.t. 3 hypergraph measures [19].

Moreover, in terms of AUROC, AHP even outperformed the variants equipped with the same sampling scheme used for each test set on 20 (out of 24) test sets. The results confirm that our adversarial training scheme significantly improves the generalization ability.

Analysis of the generator. In order to analyze how the generator evolves during training, we compared the **original hypergraph** composed of the hyperedges in the training set and the **sampled hypergraph** where 1/6 of the hyperedges in the original hypergraph were replaced by the same number of negative examples sampled by the generator. Specifically, in them, we computed the distributions of (a) **node degree** (i.e., the number of hyperedges containing each node), (b) **pair overlaps** (i.e., the number of overlapping hyperedges on each pair of nodes), and (c) **intersection size** (i.e., the number of nodes in the intersection of each pair of hyperedges), which are suggested in [19] as important hypergraph measures. As shown in Fig. 5, the distributions in the original and sampled hypergraphs became closer to each other at the 300-th epoch of training, compared to those at the first epoch. We used Kolmogorov’s D-statistic to measure the difference between distributions. The results show that the generator learned to sample negative examples closer to positive examples.

Effects of the memory bank. In two datasets, using the memory bank helped stabilizing training, as shown in Fig. 6. However, its effect on final test AUROC was marginal in all datasets except for the Pubmed dataset, where final test AUROC improved by 1.1%.

5 RELATED WORKS

Measure-based and projection-based approaches. Graph measures for edge prediction, including Katz’s index [15] and common neighbors [23], have been extended to hypergraphs for hyperedge prediction [42]. Alternatively, Yoon et al. [39] projected a hypergraph into multiple pairwise graphs and fed the graph measures on them into a machine learning model for hyperedge prediction. Zhang et al. [42] also projected a hypergraph into a pairwise graph via clique expansion and applied non-negative matrix factorization and least square matching for hyperedge prediction. This approach requires a feasible candidate set and thus inapplicable to Problem 1. **Deep learning-based approaches.** Tu et al. [32] used a neural network to estimate hyperedge formation probabilities based on

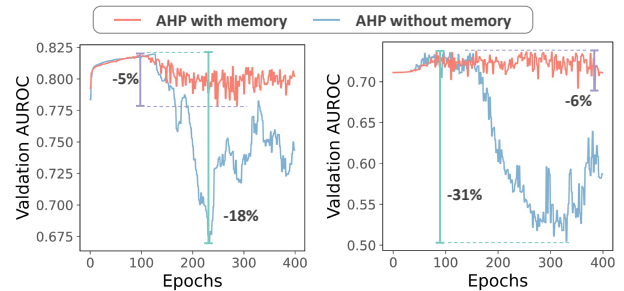


Figure 6: The effects of the memory bank in the Cora-A (left) and DBLP (right) datasets. The presented learning curves are averaged over five runs. Note that validation AUROC drops significantly without the memory bank.

node embeddings. However, it is limited to hyperedges of a fixed size. Zhang et al. [43] estimated hyperedge formation probabilities under the assumption that hyperedge-specific embeddings and general embeddings of nodes are similar within hyperedges. The discriminator of AHP, including *maxmin* pooling, is largely based on that used in [38], which applies a graph neural network [16] (and a refining step) to clique expansion for node embedding, while our discriminator uses a hypergraph neural network [10] instead.

Relation to our work. The learning-based approaches among the aforementioned ones require negative sampling, as discussed in Sect. 1. To this end, they rely on heuristics, which can be replaced by our proposed adversarial training scheme. In addition, for positive-unlabeled learning [17, 25, 36], generative adversarial networks were used to generate fake positive and/or negative examples [13, 14, 44]. To the best of our knowledge, however, none of them was applied to hypergraphs or used to generate sets.

6 CONCLUSION

In this paper, we proposed AHP, an adversarial training-based approach for hyperedge prediction. Using six real-world hypergraphs, we revealed the limited generalization capability of state-of-the-art methods, which employ heuristics for negative sampling. AHP replaces the heuristics with a learnable generator whose architecture is simple yet well-suited to hyperedge prediction. As a result, it yielded up to 28.2% higher AUROC than the best existing method, generalizing better to negative examples of various natures. Surprisingly, in most cases, AHP even outperformed its variants equipped with the same heuristics used to generate negative examples in test sets. For **reproducibility**, the code and datasets used in the paper are available at <https://github.com/HyunjinHwn/SIGIR22-AHP>.

Acknowledgements: This work was supported by National Research Foundation of Korea (NRF) grant funded by the Korea government (MSIT) (No. NRF-2020R1C1C1008296) and Institute of Information & Communications Technology Planning & Evaluation (IITP) grant funded by the Korea government (MSIT) (No. 2019-0-00075, Artificial Intelligence Graduate School Program (KAIST)).

REFERENCES

- [1] Ilya Amburg, Nate Veldt, and Austin Benson. 2020. Clustering in graphs and hypergraphs with categorical edge labels. In *WWW*.
- [2] Martin Arjovsky and Léon Bottou. 2017. Towards principled methods for training generative adversarial networks. In *ICLR*.
- [3] Martin Arjovsky, Soumith Chintala, and Léon Bottou. 2017. Wasserstein generative adversarial networks. In *ICML*.

Table 2: Details of the datasets.

	Citeseer	Cora	Cora-A	Pubmed	DBLP-A	DBLP
Category	Co-citation	Co-citation	Authorship	Co-citation	Authorship	Collaboration
Number of nodes	1,457	1,434	2,388	3,840	39,283	15,639
Number of edges	1,078	1,579	1,072	7,962	16,483	22,964
Average size of hyperedges	3.2	3	4.3	4.3	4.5	2.7
Maximum size of hyperedges	26	5	43	171	80	18
Minimum size of hyperedges	2	2	2	2	2	2
Dimension of node feature	3,703	1,433	1,433	500	4543	4543

[4] Austin R Benson, Rediet Abebe, Michael T Schaub, Ali Jadbabaie, and Jon Kleinberg. 2018. Simplicial closure and higher-order link prediction. *PNAS* 115, 48 (2018), E11221–E11230.

[5] Austin R Benson, Ravi Kumar, and Andrew Tomkins. 2018. Sequences of sets. In *KDD*.

[6] Minyoung Choe, Jaemin Yoo, Geon Lee, Woonsung Baek, U Kang, and Kijung Shin. 2022. MiDaS: Representative Sampling from Real-world Hypergraphs. In *WWW*.

[7] Hyunjin Choo and Kijung Shin. 2022. On the Persistence of Higher-Order Interactions in Real-World Hypergraphs. In *SDM*.

[8] Cazamere Comrie and Jon Kleinberg. 2021. Hypergraph Ego-networks and Their Temporal Evolution. In *ICDM*.

[9] Manh Tuan Do, Se-eun Yoon, Bryan Hooi, and Kijung Shin. 2020. Structural patterns and generative models of real-world hypergraphs. In *KDD*.

[10] Yihe Dong, Will Sawin, and Yoshua Bengio. 2020. HNHN: Hypergraph networks with hyperedge neurons. *arXiv preprint arXiv:2006.12278* (2020).

[11] Yifan Feng, Haoxuan You, Zizhao Zhang, Rongrong Ji, and Yue Gao. 2019. Hypergraph neural networks. In *AAAI*.

[12] Li He, Hongxu Chen, Dingxian Wang, Shoaib Jameel, Philip Yu, and Guandong Xu. 2021. Click-Through Rate Prediction with Multi-Modal Hypergraphs. In *CIKM*.

[13] Ming Hou, Brahim Chaib-draa, Chao Li, and Qibin Zhao. 2018. Generative Adversarial Positive-Unlabelled Learning. In *IJCAI*.

[14] Wenzheng Hu, Ran Le, Bing Liu, Feng Ji, Jinwen Ma, Dongyan Zhao, and Rui Yan. 2021. Predictive Adversarial Learning from Positive and Unlabeled Data. In *AAAI*.

[15] Leo Katz. 1953. A new status index derived from sociometric analysis. *Psychometrika* 18, 1 (1953), 39–43.

[16] Thomas N Kipf and Max Welling. 2017. Semi-supervised classification with graph convolutional networks. In *ICLR*.

[17] Ryuichi Kiryo, Gang Niu, Marthinus C Du Plessis, and Masashi Sugiyama. 2017. Positive-unlabeled learning with non-negative risk estimator. In *NIPS*.

[18] Yunbum Kook, Jihoon Ko, and Kijung Shin. 2020. Evolution of Real-world Hypergraphs: Patterns and Models without Oracles. In *ICDM*.

[19] Geon Lee, Minyoung Choe, and Kijung Shin. 2021. How Do Hyperedges Overlap in Real-World Hypergraphs? - Patterns, Measures, and Generators. In *WWW*.

[20] Geon Lee, Jihoon Ko, and Kijung Shin. 2020. Hypergraph Motifs: Concepts, Algorithms, and Discoveries. *PVLDB* 13, 11 (2020).

[21] Geon Lee and Kijung Shin. 2021. THyMe+: Temporal Hypergraph Motifs and Fast Algorithms for Exact Counting. In *ICDM*.

[22] Yicong Li, Hongxu Chen, Xiangguo Sun, Zhenchao Sun, Lin Li, Lizhen Cui, Philip S Yu, and Guandong Xu. 2021. Hyperbolic hypergraphs for sequential recommendation. In *CIKM*.

[23] David Liben-Nowell and Jon Kleinberg. 2007. The link-prediction problem for social networks. *JASIST* 58, 7 (2007), 1019–1031.

[24] Zheng Liu, Xing Xie, and Lei Chen. 2018. Context-aware academic collaborator recommendation. In *KDD*.

[25] Byeonghu Na, Hyemi Kim, Kyungwoo Song, Weonyoung Joo, Yoon-yeong Kim, and Il-Chul Moon. 2020. Deep generative positive-unlabeled learning under selection bias. In *CIKM*.

[26] Duc Anh Nguyen, Canh Hao Nguyen, and Hiroshi Mamitsuka. 2021. CentSmoothie: Central-Smoothing Hypergraph Neural Networks for Predicting Drug-Drug Interactions. *arXiv preprint arXiv:2112.07837* (2021).

[27] Prasanna Patil, Govind Sharma, and M Narasimha Murty. 2020. Negative sampling for hyperlink prediction in networks. In *PAKDD*.

[28] Kevin Roth, Aurelien Lucchi, Sebastian Nowozin, and Thomas Hofmann. 2017. Stabilizing training of Generative Adversarial Networks through regularization. In *NIPS*.

[29] Hoang Thanh-Tung, Svetha Venkatesh, and Truyen Tran. 2019. Improving generalization and stability of generative adversarial networks. In *ICLR*.

[30] Thonet Thibaut, Renders Jean-Michel, Choi Mario, and Kim Jinho. 2022. Joint Personalized Search and Recommendation with Hypergraph Convolutional Networks. In *ECIR*.

[31] Leo Torres, Ann S Blevins, Danielle Bassett, and Tina Eliassi-Rad. 2021. The why, how, and when of representations for complex systems. *SIAM Rev.* 63, 3 (2021), 435–485.

Table 3: Hyperparameter search space

Hyperparameter	Selection pool
Optimizer for the discriminator	Adam
Optimizer for the generator	Adam
Maximum epoch*	400
Learning rate for the discriminator	5e-03, 5e-04, 5e-05, 5e-06
Learning rate for the generator	1e-04, 1e-05, 1e-06, 1e-07
Normalization factor (α, β)**	(0,0), (1,1)
Memory size	0, 32, 128

(a) Search space for AHP

Hyperparameter	Selection pool
Optimizer	Adam
Learning rate	5e-02, 5e-03, 5e-04, 5e-05, 5e-06
Normalization factor (α, β)	(0,0), (1,1)
Maximum epoch*	200

*Early stopped when the validation AUROC was maximized.

** α and β are degree normalization factors of hyperedges and nodes [10].

(b) Search space for the variants of AHP

[32] Ke Tu, Peng Cui, Xiao Wang, Fei Wang, and Wenwu Zhu. 2018. Structural deep embedding for hyper-networks. In *AAAI*.

[33] Maria Vaida and Kevin Purcell. 2019. Hypergraph link prediction: learning drug interaction networks embeddings. In *ICMLA*.

[34] Oriol Vinyals, Meire Fortunato, and Navdeep Jaitly. 2015. Pointer networks. In *NIPS*.

[35] Jianling Wang, Kaize Ding, Liangjie Hong, Huan Liu, and James Caverlee. 2020. Next-item recommendation with sequential hypergraphs. In *SIGIR*.

[36] Man Wu, Shirui Pan, Lan Du, Ivor Tsang, Xingquan Zhu, and Bo Du. 2019. Long-short distance aggregation networks for positive unlabeled graph learning. In *CIKM*.

[37] Naganand Yadati, Madhav Nimishakavi, Prateek Yadav, Vikram Nitin, Anand Louis, and Partha Talukdar. 2019. HyperGCN: A New Method For Training Graph Convolutional Networks on Hypergraphs. In *NeurIPS*.

[38] Naganand Yadati, Vikram Nitin, Madhav Nimishakavi, Prateek Yadav, Anand Louis, and Partha Talukdar. 2020. NHP: Neural Hypergraph Link Prediction. In *CIKM*.

[39] Se-eun Yoon, Hyungseok Song, Kijung Shin, and Yung Yi. 2020. How Much and When Do We Need Higher-order Information in Hypergraphs? A Case Study on Hyperedge Prediction. In *WWW*.

[40] Chia-An Yu, Ching-Lun Tai, Tak-Shing Chan, and Yi-Hsuan Yang. 2018. Modeling multi-way relations with hypergraph embedding. In *CIKM*.

[41] Junwei Zhang, Min Gao, Junliang Yu, Lei Guo, Jundong Li, and Hongzhi Yin. 2021. Double-Scale Self-Supervised Hypergraph Learning for Group Recommendation. In *CIKM*.

[42] Muhan Zhang, Zhicheng Cui, Shali Jiang, and Yixin Chen. 2018. Beyond link prediction: Predicting hyperlinks in adjacency space. In *AAAI*.

[43] Ruochi Zhang, Yuesong Zou, and Jian Ma. 2020. Hyper-SAGNN: a self-attention based graph neural network for hypergraphs. In *ICLR*.

[44] Yao Zhou, Jianpeng Xu, Jun Wu, Zeinab Taghavi, Evren Korpeoglu, Kannan Achan, and Jingrui He. 2021. PURE: Positive-Unlabeled Recommendation with Generative Adversarial Network. In *KDD*.

APPENDIX

We provide in Table 2 some basic statistics from the real-world hypergraphs used in the paper. We give in Table 3 the hyperparameter search space of AHP and its variants.